



HAL
open science

Patch Graph-based Wavelet Inpainting for Color Images

David Helbert, Mohamed Malek, Pascal Bourdon, Philippe Carré

► **To cite this version:**

David Helbert, Mohamed Malek, Pascal Bourdon, Philippe Carré. Patch Graph-based Wavelet Inpainting for Color Images. *Journal of Visual Communication and Image Representation*, 2019, 64, pp.102614. 10.1016/j.jvcir.2019.102614 . hal-02271527

HAL Id: hal-02271527

<https://hal.science/hal-02271527>

Submitted on 11 Dec 2019

HAL is a multi-disciplinary open access archive for the deposit and dissemination of scientific research documents, whether they are published or not. The documents may come from teaching and research institutions in France or abroad, or from public or private research centers.

L'archive ouverte pluridisciplinaire **HAL**, est destinée au dépôt et à la diffusion de documents scientifiques de niveau recherche, publiés ou non, émanant des établissements d'enseignement et de recherche français ou étrangers, des laboratoires publics ou privés.

Patch Graph-based Wavelet Inpainting for Color Images

David Helbert^{a,*}, Mohamed Malek^b, Pascal Bourdon^a, Philippe Carré^a

^aUniv. Poitiers, CNRS, XLIM, UMR 7252, F-86000 Poitiers, France

^bENSTA-Bretagne, IT department, c2 Rue François Verny, 29806 Brest, France

Abstract

We propose a novel inpainting process for color images. Our algorithm is based on the graph-based wavelet regularization and the non-local mean approach. At each step damaged structures are estimated by computing a graph of patches and applying a regularization model using a wavelet transform on graphs. Our approach uses color information of the image to reconstruct missing data according to local geometry. We show that the graph can be used to model geometry information in the frame of inpainting and to merge candidate pixels from a graph-based wavelet regularization. We provide details on numerical approaches and the results highlight an improvement of the geometrical information reconstruction of color images.

Keywords:

2010 MSC: 00-01, 99-00

1. Introduction

Image inpainting is an interpolation problem which consists in filling-in image information in a perceptually plausible way. It can be used for reversing deterioration, film restoration, scratch, element removal, etc. For example, [1] proposed a de-interlacing algorithm for videos acquired with interlaced broadcast television formats. In the frame of the image compression, [2] proposed to decode images in recovering the non-exemplar regions with an edge-based image inpainting method. [3] used vector quantization and image inpainting to hide data in an compressed image. Recently, [4] proposed a lossy compression scheme for encrypted image. They obtained good image reconstruction results due to a total variation-based inpainting. As for [5], they suggested to reconstruct compressed flow fields in using edge-aware homogeneous diffusion inpainting.

There are a lot of works on image inpainting. Here we are interesting in the recovering of a large removed area in a color image. Despite the influence of the deep learning in image processing, we focus on graph-based modelling of color textured information.

In [6] Bertalmio proposed a propagated diffusion method based on a Partial Derivative Equations (PDE)

25 scheme to propagate information from the outside of a missing area along isophotes. A variational inpainting model is proposed by Chan and Shen using Euler Lagrange equations [7]. On the basis of realizing connectivity principle, they proposed a Curvature Driven Diffusion process [8]. While these methods are efficient to inpaint small, non-textured image regions, they are also tend to introduce blur in larger and/or textured regions thus can not maintain reasonable visual perception in the restored image. Criminisi then proposed an exemplar-based method [9] by employing a texture synthesis technique to remove a large object from an image. That consists on reconstructing missing regions from patches of an image which provide a dictionary. Recently [10] propose a Gaussian-weighted non-local texture similarity measure to give multiple candidate patches for each target patch. This method combines the multiple good candidate patches using the α -trimmed mean filter to inpaint the target patch.

To have a complete view of inpainting works, the reader can refer to the complete state of art, written by Guillemot and Le Meur [11].

However, many researchers recently work on inpainting methods using deep learning [12, 13, 14, 15, 16]. These approaches are based on model training to recover a clear image. [12] proposed to learn and predict structures in natural images using convolutional neural networks (CNNs). [17] shows that an inpainting inverse

*Corresponding author

Email address: david.helbert@xlim.fr (David Helbert)

problem can be resolved by a randomly-initialized neural network and the proposed deep image prior is sufficient to inpaint large regions.

[14] predict information in large missing regions from a trained generative model using a semantic image inpainting in deep generative modelling framework. [13] developed an on-demand learning algorithm for training image models for training deep convolutional neural networks. On the other hand, DeMeshNet is based on a feature oriented blind face inpainting [15] to clear meshes on identity photos.

Thus our approach is based on non-local information analysis of the damaged image. The aim is to argue the influence of the geometry modelling in color image inpainting processing.

Indeed, previous works have shown that the graph framework is more flexible to unify both geometry and texture based approaches. In [18] a general variational framework for image inpainting is proposed where the graph is weighted by mixing spatial and non-local information. An iteration of heat flow is then applied in order to reduce visual dissimilarities. In the next step a graph based regularization [19] is used to diffuse non-local information into the gaps. The final result is given through the repetition of the procedure. In [20] an algorithm for image and video inpainting based on a p-Laplace regularization on graph is proposed. Weights are computed taking into account local and non-local features according to the topology of the graph. The regularization process is applied iteratively on each node. This approach has shown the efficiency of the algorithm in reproducing a variable homogeneity in a complex image and the inpainting yields very good results. However these methods tend to produce blurred estimates when the removed area is very large.

While wavelet transform and patch similarity are well-known tools with a prominent place in the field of image processing but they are rarely associated within the same scheme. In this study, we have taken an interest in resolving the missing area recovery problem as an optimization problem. Thus we propose a scheme of non-local graph wavelet regularization by using the coefficients of the Spectral Graph Wavelet transform (SGWT) [21, 22] and the non-local graph.

Graph computation thereby allows to take into account color similarities in an image and have a real representation of the geometry according to color information. Candidate pixels are thus be merged to give the missing pixels from a graph-based wavelet regularization.

Note that [23] highlighted the fact that color

representation in a graph structure improves image restoration. Results of wavelet-on-graphs-based inpainting show that the proposed approach diffuses color information into missing regions. [24] proposed a signal inpainting on graphs from minimization problems and tested proposed algorithms on real-world datasets but not on color images.

In details we propose:

- a patch graph construction on known areas of the damaged image,
- a propagation of the texture through the graph construction,
- a graph-based wavelet regularization to update the missing color pixels.

We present in section 2 the graph-based representation of a color image and the principle tools of signal processing on graphs. In section 3, we present the principles of patch graph -based wavelet inpainting and we propose in section 4 to take advantage of non-local constraints in proposing an information propagation algorithm. Numerical results are given to demonstrate the efficiency of our approach in low resolution to observe the pixel value attribution.

2. Graph definition on color images

We present our notations and definitions on graphs [25, 26]. The signal on graphs and graph wavelet transform are then introduced.

2.1. Definition of a weighted graph

Any discrete domain can be represented by a weighted graph. Let $G = (V, E, w)$ be a loopless, undirected and weighted graph with V a finite set of vertices and E subset of edges $V \times V$. An edge $(m, n) \in E$ connects two vertices m and n .

The weight $w(m, n)$ of an edge (m, n) is defined by the following function:

$$w : V \times V \longrightarrow \mathbb{R}^+ \quad (1)$$

$$w(m, n) = \begin{cases} w_{mn} & \text{if } (m, n) \in E \\ 0 & \text{otherwise.} \end{cases} \quad (2)$$

Common methods are essentially based on local and non-local comparisons of features [27] and the weight function is represented by a decreasing function [28].

Let \mathbf{A} be the weighted adjacency matrix of size $N \times N$ with N the number of vertices. Adjacency matrix is defined as follow:

$$\mathbf{A}_{m,n} = \begin{cases} w(m,n) & \text{if } (m,n) \in E \\ 0 & \text{otherwise.} \end{cases} \quad (3)$$

The degree of a vertex m is defined as the sum of the weights of all adjacent vertices to m in the graph. We also define degree matrix \mathbf{D} as a diagonal matrix of the vertex degrees.

2.2. Graph construction from color information

Let \mathbf{f} be a signal on graph. \mathbf{x}_m denotes the embedding of graph G of the image on a 2-dimensional Euclidean space and \mathbf{f}_m are the embedding of G on a color RGB space for vertex m .

The graph connects corresponding pixels with the same color similarities. Each pixel also corresponds to a vertex. Therefore the graph is obtained by computing the k -Nearest Neighbour algorithm according to similarity measures between the color of vertex pairs. The correspondence between two vertices m and n can be evaluated through a similarity measure $\rho_{m,n}$. However, a color similarity measure can be introduced in the graph building by defining a color-based structure.

We propose to compute data-driven weights $w_{m,n}$ between vertex pairs (m, n) which depend on color similarity measures $\rho_{m,n}$ between \mathbf{f}_m and \mathbf{f}_n [29]. The weights are given by:

$$w_{m,n} = \exp\left(\frac{-\rho_{m,n}^2}{2\sigma_f^2}\right), \quad (4)$$

where σ_f adjusts the influence of color information during similarity computation.

2.3. Spectral graph wavelet transform

We focus on regularization in the graph-wavelet domain by using the Spectral Graph Wavelet Transform (SGWT) proposed by Hammond *et al* in [21]. Aside from the flexibility and easy implementation of the SGWT, graph construction can drive the analysis and reconstruction process depending on connections.

The Laplacian graph of G is denoted by:

$$\mathcal{L} = \mathbf{D} - \mathbf{A}, \quad (5)$$

where \mathbf{A} and \mathbf{D} denote respectively the adjacency matrix and the degree matrix. By analogy, the eigenvectors of \mathcal{L} noted by χ_l with $l = 0, \dots, N-1$ form an orthonormal basis for the graph spectral domain. We have:

$$\mathcal{L}\chi_l = \Lambda_l\chi_l, \quad (6)$$

where Λ_l is a non negative eigenvalue, $\Lambda_0 = 0 \leq \Lambda_1 \leq \dots \leq \Lambda_{N-1}$.

The graph Fourier transform of \mathbf{f} is defined by:

$$\hat{\mathbf{f}} = \mathbf{X}^T \mathbf{f}, \quad (7)$$

with \mathbf{X} a matrix whose columns are the eigenvectors of the graph Laplacian \mathcal{L} . The graph wavelet operator at a given scale t is defined by $T_g^t = g(t\mathcal{L})$. The wavelet kernel $g(x)$ is considered as a band pass function. The wavelet coefficient W_f of spectral plane $\hat{\mathbf{f}}^l$ at wavelength λ and scale t is defined as follows:

$$W_{\mathbf{f}}(t, n) = (g(t\mathcal{L})\mathbf{f})(n) = \sum_l g(t\lambda_l) \hat{\mathbf{f}}(l) \chi_l(n), \quad (8)$$

and the scaling function coefficient S_f :

$$S_{\mathbf{f}}(n) = (h(\mathcal{L})\mathbf{f})(n) = \sum_l h(\lambda_l) \hat{\mathbf{f}}(l) \chi_l(n), \quad (9)$$

with $h(x)$ a low pass function satisfying $h(0) > 0$ and $\lim_{x \rightarrow \infty} h(x) = 0$.

Mathematical properties and the numerical implementation of the SGWT are detailed in [21].

3. Patch graph based wavelet inpainting

We propose an inpainting procedure where information deterred from a graph of patches is merged together with a sparse regularization scheme, and improved through a numerical diffusion process.

3.1. Sparse regularization scheme for wavelet inpainting

In this part we present in a general way an approach for inpainting by sparse regularization [30].

Let $\mathbf{r} \in \mathbb{R}^N$ be the observed color signal of size N and $\mathbf{f} = \Phi \mathbf{r} + \mathbf{n}$ the signal with missing pixels at locations Φ with $\mathbf{n} \in \mathbb{R}^N$ an additive noise. By definition, \mathbf{r} is sparse in the dictionary Ψ^* (synthesis operator) and is obtained through a linear combination $\mathbf{r} = \Psi^* \mathbf{a}$. We compute a sparse set of coefficients \mathbf{a} in a frame $\Psi = (\psi_m)$:

$$\hat{\mathbf{a}} = \underset{\mathbf{a}}{\operatorname{argmin}} \frac{1}{2} \|\mathbf{f} - \Phi \Psi^* \mathbf{a}\|_2^2 + \gamma R(\mathbf{a}), \quad (10)$$

where $R(\mathbf{a}) = \sum_n |\mathbf{a}_n|$ is the ℓ_1 -sparsity regularizer and $\gamma \in \mathbb{R}$ a noise-dependent value.

The optimization problem defined in Eq. 10 is known as an ill-posed inverse problem. In [30] it is solved with an iterative soft thresholding operator \mathcal{T}_γ^S ¹, with

¹Soft thresholding is defined by: $\mathcal{T}_\gamma^S(d_{i,k}) = \operatorname{sign}(d_{i,k}) (|d_{i,k}| - \gamma)_+$ and if $a < 0$ then $(a)_+ = 0$ else $(a)_+ = a$.

195 threshold $\gamma \in \mathbb{R}$. The numerical scheme is presented in Algo. 1. A robust estimate of γ can be the median absolute deviation on the first scale of the wavelet decomposition [31].

Algorithm 1: *WInpainting()*: Wavelet Inpainting process.

Input: $\mathbf{f}, \Psi, \Phi, \epsilon$
Result: \mathbf{r}
begin
 $\mathbf{y}_0 \leftarrow \mathbf{f};$
 $k \leftarrow 0;$
 repeat
 $\mathbf{y}_{k+1} \leftarrow \mathbf{y}_k + \Phi \left[\Psi^* \mathcal{T}_\alpha^S \Psi \mathbf{y}_k - \mathbf{y}_k \right];$
 $k \leftarrow k + 1;$
 until $\sum (\mathbf{y}_{k+1} - \mathbf{y}_k)^2 < \epsilon;$
 $\mathbf{r} \leftarrow \mathbf{y}_{k+1};$

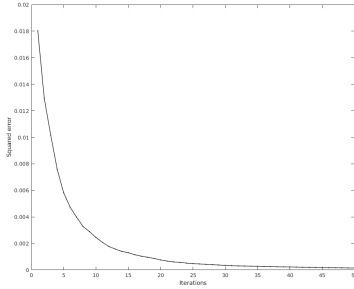


Figure 1: Iterative process: squared error between two consecutive images.

Fig 1 illustrates the error convergence during the iterative process. So we set the error threshold $\epsilon = 5 \times 10^{-4}$.

200 In this Algo. 1 we can use a classical discrete wavelet transform or a graph-based wavelet transform with wavelet function obtained from the graph Laplacian matrix.

3.2. Patch graph construction

205 Buades *et al* developed the concept of non-local means for image denoising [27]. They assume that the image contains an extensive amount of self-similarity and extensive amount of redundancy which can then be exploited to remove noise in the image. They integrate a non-locality factor into a variational problem. 210 The graph framework can also design to easily integrate such a constraint. Davov *et al* proposed the BM3D, a collaborative filtering based on the grouping of similar patches in a 3D block and a denoising process [32].

We propose to adopt the non-local concept in graph computation in [18]. We use the input image to compute the non-local graph. The weight of two given vertices m and n is computed by considering two square patches Γ_m and Γ_n of size $a \times a$ centered on the spatial coordinates of m and n ; a is odd. We compute weights $\rho_{m,n}$ using all similarity measures between patch pairs:

$$\rho_{m,n} = \sqrt{\sum_{i=1}^{a^2} d(\mathbf{f}_{m+i}, \mathbf{f}_{n+i})}. \quad (11)$$

215 where d is the Euclidean distance. [23] suggested different similarity measures to construct the graph in particular a perceptual distance and the Euclidean distance. We choose these last one because of the low computational cost.

220 Although the non-local graph is an interesting modelling tool, it requires a computationally efficient algorithm. In Algo. 2, we compute similarity measures in a restricted patch neighbourhood \mathbf{B}_m of size $b \times b$. Known patches in the region \mathbf{B}_m are so connected to vertex m .

Algorithm 2: *WeightComputation()*: Weight computation on region Θ .

Input: Θ, a, b
Result: \mathbf{A}
begin
 for $m \in \Theta$ **do**
 Define patch Γ_m of size $a \times a$;
 Define windows \mathbf{B}_m ;
 for $n \in \mathbf{B}_m$ **do**
 Define patch Γ_n of size $a \times a$;
 Compute $\rho_{m,n}$ with Eq. 11;
 Compute $\omega_{m,n}$ with Eq. 4;
 $\mathbf{A}_{m,n} \leftarrow \omega_{m,n};$

3.3. Inpainting results

225 We consider a color image \mathbf{f} with a damaged area Φ and denote $\mathbf{A}_{m,n}$ the weights between vertices m and n .

230 Starting the inpainting process, we compute the graph of patches using non-missing pixels of the image. Therefore we propose to estimate pixel adjacencies of damaged area subsets before regularizing.

Note that despite applying the regularization process on each color plane, our approach is not marginal. Indeed, color information is modelled within a graph.

235 We evaluate the recovering process on a 64×64 image with a 28×28 damaged zone (see Fig. 2(a)) with following wavelet-based inpainting:

- a discrete wavelet transform with a relaxed orthogonality constraint, namely the Undecimated Wavelet Transform (UWT) Daubechies D8 (see Fig. 2(b)),
- a graph wavelet approach (see Fig. 2(c)). The graph are computed with 4-nearest neighbors (Cartesian grid).
- a patch-based graph wavelet approach (see Fig. 2(d)), where wavelet transform is computed with Algo. 2. The missing region is considerate as a Cartesian grid in the graph computation.

To threshold the undecimated wavelet coefficients, we empirically use a linear decreasing function from 500 to 1 on 500 iterations. From the graph-based wavelet approach, we compute the graph Laplacian and then wavelet filters.

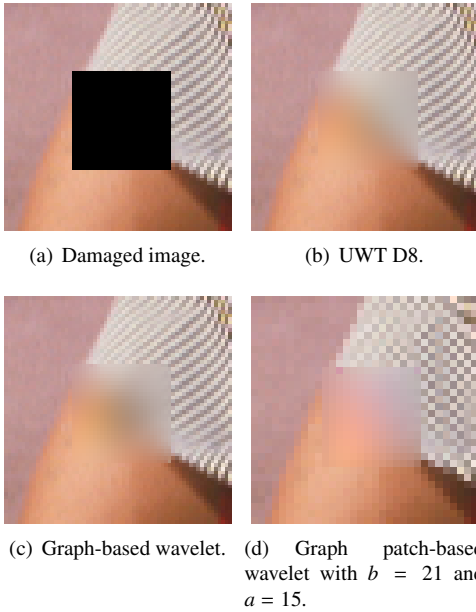


Figure 2: Wavelet-based recovering processes on an edge.

Fig. 2(b) shows that UWT-based image reconstruction does not reconstruct geometric information. Fig. 2(c) highlights the same smoothing effect. The regularization process mixes color pixels values with weights which correspond to the similarity values; false colors thus appear.

To reconstruct a missing data with a graph wavelet transform, the graph should take into account texture information. Thus we propose to connect vertices which are centered on a similar texture and to compute the similarity measurement between patches. Moreover we

propose a solution to compute the graph inside a missing region during the regularization process.

4. Propagation of geometrical information

4.1. Principle

Exemplar-based approaches promote Gaussian pyramids to recover large damaged areas [9]. Here we want to show that color information can be propagated into the graph structure as shown Fig. 3. The global process is illustrated on Fig. 4.

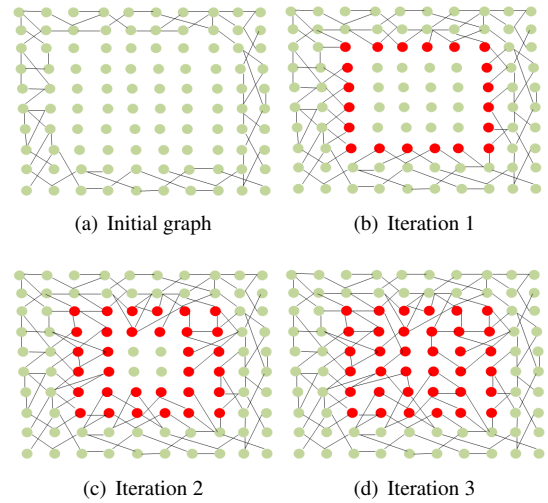


Figure 3: Information propagation principle through the graph construction.

The main idea is also to synthesize iteratively a set of pixels \mathcal{E}_i of the damaged area Φ before regularizing. This method is effective to infer the missing data.

Let C_i be a set of pixels. The union of K sets C_i has to form the damaged zone $\Phi = \bigcup_{i=1}^K C_i$. A numerical solution is to define the set C_1 as a inner contour of the damaged zone and to define the others by contraction. We denote $\mathcal{E}_i = \bigcup_{k=1}^i C_k$ as the set of processed pixels at iteration i (see Fig. 5). At each iteration, we update the graph of patches by adding the non-local structure associated to set C_i .

For the first contour we have $\mathcal{E}_1 = C_1$. We estimate the missing structure by using the non-local graph computation, other vertices of the damaged area are not connected. We initialize the missing coefficients of vertex m of the signal on graph \mathbf{f} by the pixel value centered on the most similar patch Ω_m^* that can be written as follow-

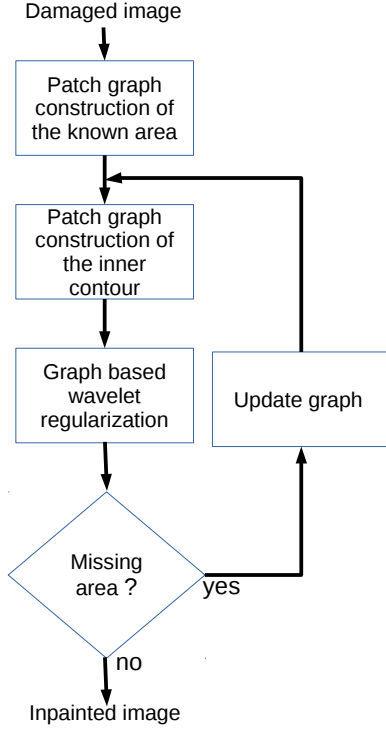


Figure 4: Global scheme of the inpainting process.

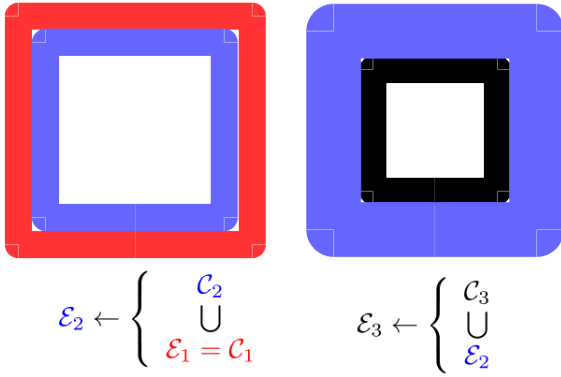


Figure 5: Definition of processed pixel sets.

ing:

$$\Omega_m^* = \arg \min_{\Omega_n \in B_m} \rho_{m,n} \quad (12)$$

$$\mathbf{f}_m = \Omega_m^* \left(\left\lceil \frac{a^2}{2} \right\rceil \right) \quad (13)$$

with $\lceil \cdot \rceil$ the ceiling function. Algorithm 3 illustrates the process for a set C_i of missing pixels.

The graph-based wavelet regularization is then applied and regularized \mathcal{E}_1 is now considered as known

Algorithm 3: *PixelInit()*: Initialization of missing pixels.

Input: \mathbf{f}, C_i, a, b

Result: \mathbf{f}

begin

for $m \in C_i$ **do**

$\Omega_m^* \leftarrow \arg \min_{\Omega_n \in B_m} \rho_{m,n}$;

$\mathbf{f}_m \leftarrow \Omega_m^* \left(\left\lceil \frac{a^2}{2} \right\rceil \right)$;

end

data. Wavelet transform are calculated on 4 scales.

We process the next iteration and set \mathcal{E}_2 is defined by $\mathcal{E}_2 = C_1 \cup C_2$ and we apply the same processing (see Fig. 5).

In each step, data on contour $C_i = C_{i-1} \cup \mathcal{E}_i$ is reconstructed by regularizing the processed area \mathcal{E}_i (see Algo. 4). Pixels on missing contour C_i have finally new color information, we compute the new vertex pair weights and the graph adjacency matrix is thus updated.

Note that the total number of iterations depends on the size of Φ and that recovered pixel values change when the processing iterates.

This procedure iterates several times until the missing area becomes empty.

Missing areas here are rectangular and contour extractions and contractions are based on the classical binary mathematical morphology operators. Note that the damaged area can take any shape. The choice of patch size is an important consideration. It must be large enough in order to get a relevant comparison of features. The success is insured by the regularity measured in the spectral graph wavelet domain.

4.2. Results and discussion

4.2.1. Evaluation of the color inpainting process

We evaluate the performance of the proposed inpainting processing. We compare the proposed recovering process with exemplar-based inpainting [9] and generative image inpainting [16] (deep learning based approach). Both methods are considered as references in the literature. We compute two quality indices between the reconstructed regions and the original ones:

- the statistical measure Signal-to-Noise Ratio (SNR),
- the structural similarity indices (SSIM) [33].

We generate 50 damaged areas Φ of size 28 by 28 pixels at random positions on the following color images: *Barbara* (see Fig. 6(a)), *Lenna* (see Fig. 6(b)),

Algorithm 4: *PGWinpainting()*: Patch graph based wavelet inpainting algorithm with mask redefinition.

Input: $f, \Phi, niter$
Result: \mathbf{r}
begin
 // Adjacencies for known pixels
 $\mathbf{A}_1 \leftarrow \text{WeightComputation}(f - \Phi, a, b);$
 // Extraction of the first contour
 Extract contour C of on mask Φ ;
 $\mathcal{E} \leftarrow \{\emptyset\};$
 while $C \neq \{\emptyset\}$ **do**
 Concatenate C into \mathcal{E} ;
 // Adjacency computation for missing pixels
 $\mathbf{A}_2 \leftarrow \text{WeightComputation}(C, a, b);$
 Compute \mathcal{L} from $\mathbf{A}_1 + \mathbf{A}_2$;
 Compute wavelet filters from \mathcal{L} ;
 $\mathbf{f} \leftarrow \text{PixelInit}(\mathbf{f}, C, a, b);$
 // Graph wavelet regularization
 for $\lambda \in \{R, G, B\}$ **do**
 $\mathbf{f}^\lambda \leftarrow \text{WInpainting}(\mathbf{f}^\lambda, \Psi, \mathcal{E}, niter)$
 ;
 // New adjacency computation for the set of updated pixels
 $\mathbf{A}_2 \leftarrow \text{WeightComputation}(\mathcal{E}, a, b);$
 $\mathbf{A}_1 \leftarrow \mathbf{A}_1 + \mathbf{A}_2$;
 Contract Φ ;
 Extract contour c of on mask Φ ;
 $\mathbf{r} \leftarrow \mathbf{f};$

Peppers (see Fig. 6(c)), *Peppers* (see Fig. 6(d)) and *Girl* (see Fig. 6(e)) of size 512 by 512 pixels.

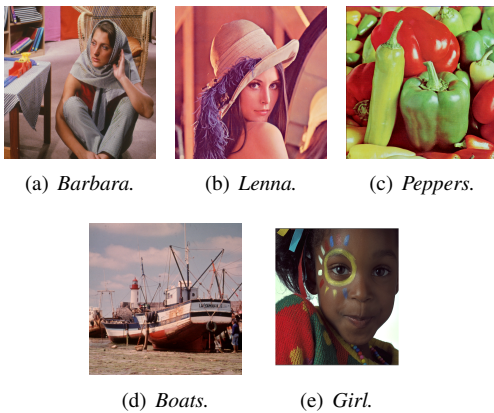


Figure 6: Images.

We fix parameter b of research region B_m to 15 and a of patch to 7. Results of quality evaluations are given in Tab. 1.

Tab. 1 proves the significant improvement of our inpainting approach. The generative inpainting method gives best Signal-Noise Ratios. However, our Patch Graph Wavelet Inpainting has best results in terms of Structural SIMilarity index (SSIM)[33]. Exemplar-based method gets worse snr results unlike our inpainting method bur SSIM indices are closed to our proposed method. Indeed the missing region size is not enough high to benefit the exemplar-based method performance.

Following illustrations will explain the difference between SNR and SSIM indices for the generative inpainting.

4.2.2. Influence of graph construction

To evaluate the inpainting processing, we choose to observe the modification of color pixel values on limited zones.

We fix parameter b of research zone B_m to 29 for all the following processes. For this experimentation, the size of patch a is equal to 7.

The computed color value of a missing pixel is obtained by a diffusion of color information according to vertices. The final value is a mix of color information of said connected vertices.

Parameter σ_f influences graph construction. When σ_f increases, weight $w_{m,n}$ between two vertices increases (up to 1). In such a case color information has a lesser influence on the discrimination of patch pairs. Patches can be considered as close, therefore the regularization process will merge color information. We observe this artefact on Fig. 7(f) with false colors appearance.

If σ_f is low, vertices of similar patches will be connected and color information of other patches tend to diffuse into the damaged area. For a lower value of $\sigma_f = 0.1$, there is a little diffusion (see Fig. 7(d)).

Better results are given with $\sigma_f = 0.25$ (see Fig. 7(e)).

4.2.3. Influence of patches

Now the missing area is placed on ruptures between a strongly textured zone and a homogeneous one (see Fig. 7(a)). We compare reconstructions using two patch sizes: $a = 7$ and 11. A value equal to 11 is high enough to discriminate two textures in our test image.

Fig. 8(c) shows a result without regularizing. Having a graph of patches, we regularize it with a simple SGWT-based regularization (see Fig. 8(a)). We observe

		<i>Barbara</i>			<i>Lenna</i>		
		Criminisi	Generative	PGWI	Criminisi	Generative	PGWI
SNR	Mean	15,38	15,66	16,04	14,99	17.53	16,15
	SD	6,83	5.97	6,43	4,55	3.47	4,60
	Median	12,83	14.86	13,38	13,98	17.28	16,89
SSIM	Mean	0,88	0.50	0,90	0,80	0.64	0,82
	SD	0,10	0.25	0,10	0,05	0.15	0,09
	Median	0,91	0.41	0,92	0,80	0.66	0,84

		<i>Peppers</i>			<i>Girl</i>		
		Criminisi	Generative	PGWI	Criminisi	Generative	PGWI
SNR	Mean	14,09	17.676	15,12	12,90	13.82	13,44
	SD	2,3	3.27	2,27	3,02	9.77	2,90
	Median	15,39	17.64	16,70	12,14	13.45	13,17
SSIM	Mean	0,80	0.68	0,81	0,91	0.43	0,92
	SD	0,04	0.15	0,03	0,08	0.24	0,08
	Median	0,78	0.65	0,82	0,95	0.40	0,97

Table 1: Signal-to-noise ratios (SNR) and structural similarity indices (SSIM) of reconstructed areas: Criminisi[9], generative inpainting[16], Patch Graph Wavelet Inpainting (PGWI)

a block artefact appearance because of mask edges. A smoothing effect on homogeneous areas is also observed.

Propagating and updating missing pixels by graph wavelet regularization allow a better reconstruction (see Fig. 8(d) and 8(f)). We also observe the appearance of false colors on edges on Fig. 8(f) while geometric information is better reconstructed.

On Fig. 8(b), we observe that the generative image inpainting reconstructs the missing area with a smoothing effect.

4.2.4. Illustrations on the process in other cases

In Fig. 9(a), a missing area is placed on an edge (see Fig. 9(b)). In this case we see on Fig. 9(e) an error of estimation of the initial pixel which propagates in the next steps. The regularization on graphs that we see on Fig. 9(f) demonstrates a good structure coherence. On Fig. 9(d), the generative inpainting [16] reconstructs the principal contour without others details.

The missing area is placed on a rupture between a strongly textured zone and a red one (see Fig. 10(b)). The red zone is composed of homogeneous zones with close colors. The regularization allows to obtain a more realistic reconstruction (see Fig. 10(f)). On Fig. 10(d), the reconstructed red zones have hard edges and grey lines appear because of faulty pixel value initialization. On Fig. 10(e), the generative inpainting [16] does not reconstruct textures and add false colors (blue) in the zebra texture.

The results on Fig. 11 show performance of graph-based wavelet inpainting on image *Bungee* [6]. The propagation process corrects missing color pixel values; we improve the color texture recovering. Graph construction allows to propagate color information according to geometrical structures. The patch size has to be chosen to discriminate texture information. The exemplar-based inpainting gives a good result but we observe on Fig. 11(b) that the house is separated in two parts. As for the generative inpainting[16] on Fig. 11(c), the roof of the house is correctly reconstructed but with a smoothing effect on textured zones.

The disadvantage of our approach lies in the need to calculate an Eigendecomposition of a large Laplacian matrix. Indeed an image of size 128×128 needs a Laplacian matrix of size $128 * 128 \times 128 * 128$ or 2 Gigabytes in double-precision floating-point format. The Laplacian matrix for an image of size 256×256 needs also 32 Gigabytes in memory. Thus the computation time for the inpainting of an image of size 128×128 and a missing which is closed to 5 minutes on a laptop with Matlab, a Linux OS and an Intel(R) Core(TM) i7-7560U CPU at 2.40 GHz without processing on GPU.

5. Conclusion

In this article, we presented a novel wavelet-based algorithm for color image inpainting by modelling images

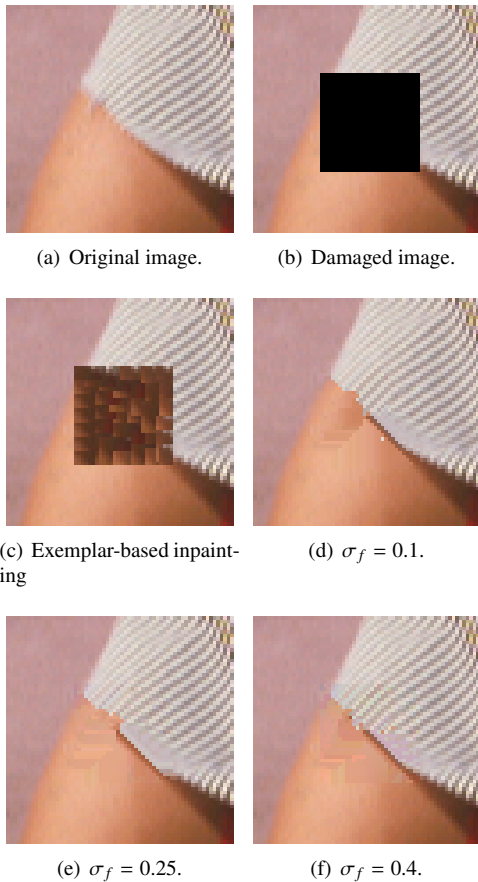


Figure 7: Influence of graph computation on image *Barbara* by patch graph wavelet inpainting with patches of size 7×7 .

on graphs. We have tested global wavelet-based inpainting methods and we have illustrated their smoothing effects in the texture reconstruction. We have proposed to use a non-local approach and a propagation of color information. We estimate the global geometry of missing data by computing a graph of patches.

We take into account color and geometrical information to infer the damaged area through the graph wavelet regularization. During a propagation process, missing color pixels are calculated and patch graphs are updated. Associating graph-based wavelet regularization with structure propagation allows to give good inpainting results. We have shown that it can correct missing pixel values to improve color texture perception.

Despite the memory cost of our approach, experimental results focus on the assignment of missing color pixels, we locally observe significant improvements; discontinuities between color and textured regions are well reconstructed and the resulting images are visually co-

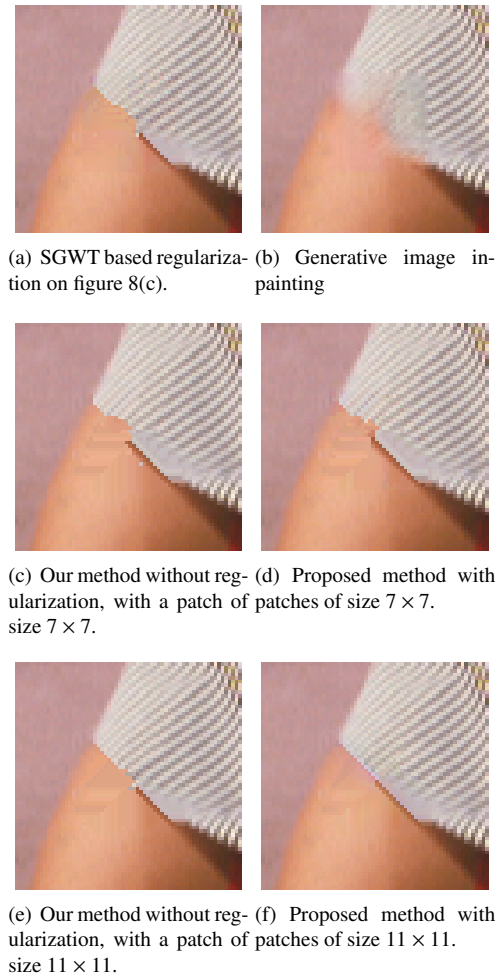


Figure 8: Influence of the patch size on image *Barbara*.

herent.

References

- [1] C. Ballester, M. Bertalmío, V. Caselles, L. Garrido, A. Marques, F. Ranchin, An inpainting-based deinterlacing method, *IEEE Transactions on Image Processing* 16 (2007) 2476–2491.
- [2] D. Liu, X. Sun, F. Wu, S. Li, Y.-Q. Zhang, Image compression with edge-based inpainting, *IEEE Transactions on Circuits and Systems for Video Technology* 17 (2007) 1273–1287.
- [3] C. Qin, C.-C. Chang, Y.-P. Chiu, A novel joint data-hiding and compression scheme based on smvq and image inpainting, *IEEE transactions on image processing* 23 (2013) 969–978.
- [4] C. Qin, Q. Zhou, F. Cao, J. Dong, X. Zhang, Flexible lossy compression for selective encrypted image with image inpainting, *IEEE Transactions on Circuits and Systems for Video Technology* (2018).
- [5] F. Jost, P. Peter, J. Weickert, Compressing flow fields with edge-aware homogeneous diffusion inpainting, *arXiv preprint arXiv:1906.12263* (2019).

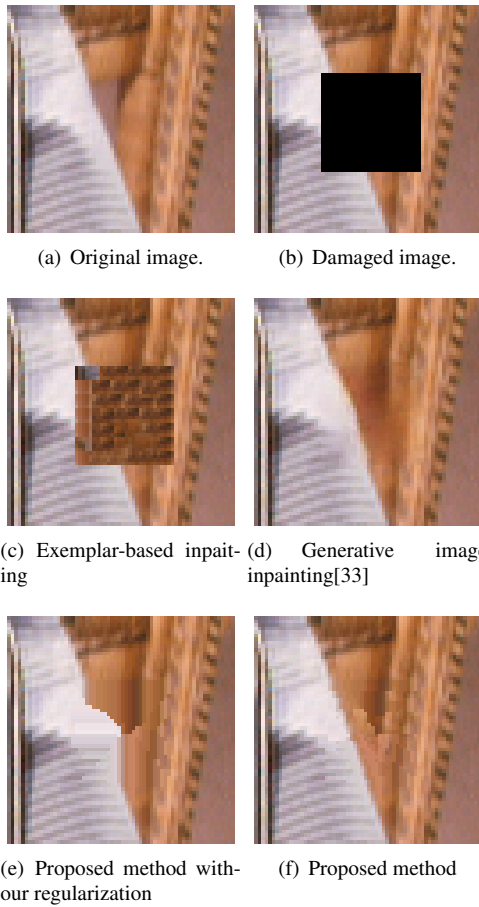


Figure 9: Inpainting processing on image *Barbara* with a patch of size 7×7 .

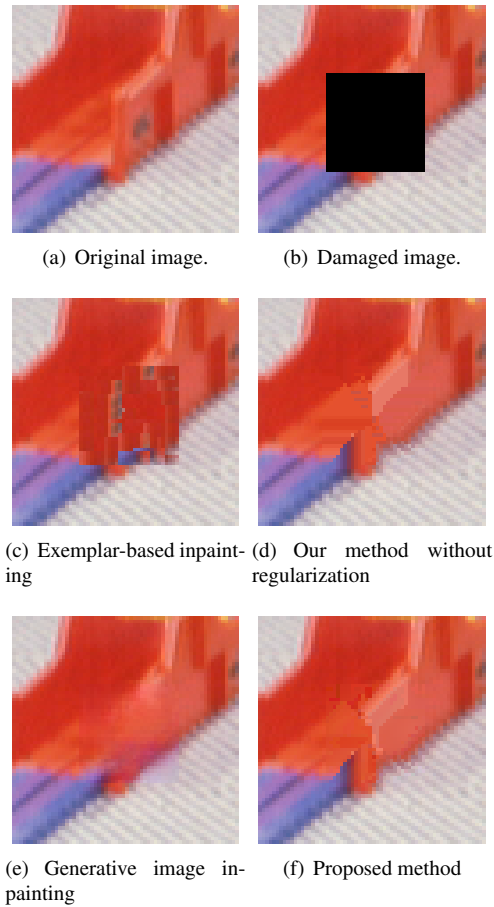


Figure 10: Inpainting processing on image *Barbara* with a patch of size 9×9 .

- [6] M. Bertalmio, G. Sapiro, V. Caselles, C. Ballester, Image inpainting, in: Proceedings of the 27th Annual Conference on Computer Graphics and Interactive Techniques, SIGGRAPH '00, ACM Press/Addison-Wesley Publishing Co., New York, NY, USA, 2000, pp. 417–424.
- [7] T. Chan, J. Shen, Mathematical models for local nontexture inpaintings., *SIAM J. Appl. Math* 62 (2002) 1019–1043.
- [8] T. Chan, J. Shen, Nontexture inpainting by curvature-driven diffusions., *J. Vis. Commun. Image Represent.* 12 (2001) 436–449.
- [9] A. Criminisi, P. Perez, K. Toyama, Region filling and object removal by exemplar-based image inpainting, *IEEE Trans. on Image Processing* 13 (2004) 1200–1212.
- [10] D. Ding, S. Ram, J. J. Rodriguez, Image inpainting using nonlocal texture matching and nonlinear filtering, *IEEE Transactions on Image Processing* 28 (2019) 1705–1719.
- [11] C. Guillemot, O. Le Meur, Image inpainting: Overview and recent advances, *IEEE signal processing magazine* 31 (2014) 127–144.
- [12] D. Pathak, P. Krahenbuhl, J. Donahue, T. Darrell, A. A. Efros, Context encoders: Feature learning by inpainting, in: Proceedings of the IEEE Conference on Computer Vision and Pattern Recognition, 2016, pp. 2536–2544.
- [13] R. Gao, K. Grauman, On-demand learning for deep image restoration, in: Proc. IEEE Conf. Comput. Vision and Pattern Recognition, 2017, pp. 1086–1095.
- [14] R. A. Yeh, C. Chen, T. Y. Lim, A. G. Schwing, M. Hasegawa-Johnson, M. N. Do, Semantic image inpainting with deep generative models, in: Proceedings of the IEEE Conference on Computer Vision and Pattern Recognition, 2017, pp. 5485–5493.
- [15] S. Zhang, R. He, Z. Sun, T. Tan, Demeshnet: Blind face inpainting for deep meshface verification, *IEEE Transactions on Information Forensics and Security* 13 (2018) 637–647.
- [16] J. Yu, Z. Lin, J. Yang, X. Shen, X. Lu, T. S. Huang, Generative image inpainting with contextual attention, in: Proceedings of the IEEE Conference on Computer Vision and Pattern Recognition, 2018, pp. 5505–5514.
- [17] V. Lempitsky, A. Vedaldi, D. Ulyanov, Deep image prior, in: 2018 IEEE/CVF Conference on Computer Vision and Pattern Recognition, 2018, pp. 9446–9454. doi:10.1109/CVPR.2018.00984.
- [18] E. D’Angelo, P. Vanderghyest, Towards unifying diffusion and exemplar-based inpainting, in: International Conference On Image Processing, IEEE, 2010, pp. 417–420.
- [19] O. Lezoray, A. Elmoataz, S. Bougleux, Graph regularization for color image processing, *Computer Vision and Image Under-*

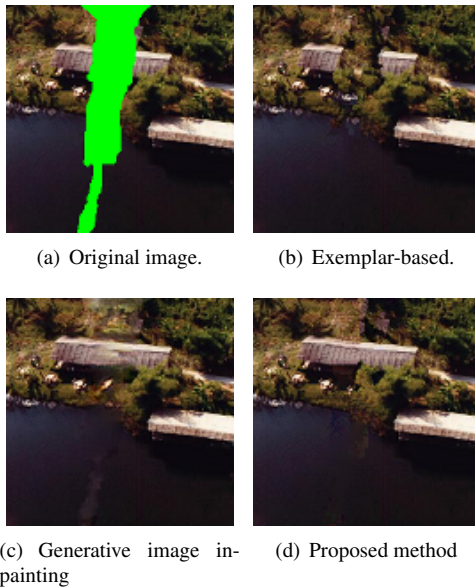


Figure 11: Inpainting processing on image *Bungee* of size 128×128 with a patch size 7×7 .

- standing 107 (2007) 38–55.
- [20] M. Ghoniem, Y. Chahir, A. Elmoataz, Nonlocal video denoising, simplification and inpainting using discrete regularization on graphs, *Signal Processing* 90 (2010) 2445–2455.
- [21] D. K. Hammond, P. Vandergheynst, R. Gribonval, Wavelets on graphs via spectral graph theory, *Applied and Computational Harmonic Analysis* 30 (2011) 129–150.
- [22] D. K. Hammond, L. Jacques, P. Vandergheynst, image denoising with nonlocal spectral graph wavelets, in: *Image Processing and Analysis with Graphs: Theory and Practice*, CRC Press, 2012.
- [23] M. Malek, D. Helbert, P. Carré, The perceptual wavelet transform based on graphs., *Journal of Electronic Imaging* 24 (2015).
- [24] S. Chen, A. Sandryhaila, J. M. Moura, J. Kovačević, Signal recovery on graphs: Variation minimization, *IEEE Transactions on Signal Processing* 63 (2015) 4609–4624.
- [25] F. R. Chung, *Spectral graph theory*, volume 92, American Mathematical Soc., 1997.
- [26] D. Spielman, *Spectral graph theory*, in: U. Naumann, O. Schenk (Eds.), *Combinatorial Scientific Computing*, CRC Press, 2012, pp. 495–524.
- [27] A. Buades, B. Coll, J.-M. Morel, Nonlocal image and movie denoising, *International journal of computer vision* 76 (2008) 123–139.
- [28] L. Grady, M.-P. Jolly, Weights and topology: A study of the effects of graph construction on 3d image segmentation, in: *Medical Image Computing and Computer-Assisted Intervention—MICCAI 2008*, Springer, 2008, pp. 153–161.
- [29] A. Gadde, S. K. Narang, A. Ortega, Bilateral filter: Graph spectral interpretation and extensions, in: *Image Processing (ICIP), 2013 20th IEEE International Conference on*, IEEE, 2013, pp. 1222–1226.
- [30] I. Daubechies, M. Defrise, C. De Mol, An iterative thresholding algorithm for linear inverse problems with a sparsity constraint, *Communications on pure and applied mathematics* 57 (2004) 1413–1457.
- [31] D. L. Donoho, J. M. Johnstone, Ideal spatial adaptation by wavelet shrinkage, *Biometrika* 81 (1994) 425–455.
- [32] K. Dabov, A. Foi, V. Katkovnik, K. Egiazarian, Image denoising by sparse 3-d transform-domain collaborative filtering, *IEEE Transactions on image processing* 16 (2007) 2080–2095.
- [33] Z. Wang, A. C. Bovik, H. R. Sheikh, E. P. Simoncelli, Image quality assessment: from error visibility to structural similarity, *IEEE transactions on image processing* 13 (2004) 600–612.